Temperature-Dependent Changes in the Structure of the Amorphous Domains of Semicrystalline Polymers

Marc L. Mansfield

Michigan Molecular Institute, Midland, Michigan 48640. *Received September 29, 1986*

ABSTRACT: There is experimental evidence for transport between the two phases of semicrystalline polymers: The change in degree of crystallinity accompanying isothermal crystal thickening and the change in domain thickness recently observed by Tanabe, Strobl, and Fischer are two examples. If transport occurs, a state of local equilibrium must exist between the two phases in which the chemical potentials of the two phases are matched. This can only occur if the structure of the amorphous domains adjusts to changes in temperature, which in turn implies that the amorphous domains are structurally different from the bulk melt. The match in chemical potentials is achieved when rubber elasticity forces pulling bonds out of the crystal are balanced by the thermodynamic driving force pulling bonds out of the melt. Large changes in domain thickness and chain anisotropy are predicted as the system is heated from room temperature to near the melting point, in agreement with the Tanabe–Strobl–Fischer measurements. We predict that this state of local equilibrium is achieved in times of about 1 s in polyethylene at temperatures for which the α relaxation is active. We attempt to reconcile these results with evidence suggesting that the amorphous domains are structurally equivalent to the bulk melt.

Introduction

A certain body of evidence,[2] mainly infrared and Raman vibrational data, supports the widely accepted notion that the amorphous phase of semicrystalline polymers is structurally equivalent to the bulk melt. This requires that the chemical potentials of the two phases are unequal, since equality only holds at the transition temperature. However, there is also good evidence that, at least at certain temperatures, transport is possible between the amorphous and crystalline phases. For example, the crystalline α relaxation is generally accepted to be due to reptation of polymer stems within the crystal,[3-11] which would, of course, permit transport. Even if our conception of the α relaxation is incorrect, or if we are concerned with one of the many polymers that does not exhibit an α relaxation, the change in degree of crystallinity accompanying isothermal crystal thickening[12,13] and the change in crystal or amorphous domain thickness observed by Tanabe et al.[1] indicate transport. Since transport occurs between the two phases, a state of local equilibrium exists in which the chemical potentials of the two phases are matched. This argument demonstrates that the amorphous domains cannot be structurally equivalent to the bulk melt.

The inability of the system to reach equilibrium has always been attributed to the entangled state of the amorphous phase. Two forces are present that control the net transport of matter from one phase to the other, namely the force of rubber elasticity due to the entangled amorphous network of chains and the thermodynamic driving force toward crystallization. If we assume transport between the two phases, then it is natural to assume that a two-phase local equilibrium exists in which these two forces are balanced, i.e., for which the chemical potentials of the two phases are matched. As the temperature changes, the structure of the amorphous domains should adjust to maintain equality of the chemical potentials.

Tanabe, Strobl, and Fischer[1] have recently published SAXS line-shape analyses that indicate large changes in the thickness of the crystalline and amorphous domains of polyethylene with changing temperature. They find that the amorphous domains change in thickness from about 30 Å at room temperature to about 150 or 200 Å near the melting point.[14] This change in thickness occurs nearly reversibly, with only some indication of hysteresis at higher temperatures. We assert in this paper that the change in thickness is produced by the balance between the two forces mentioned above. Tanabe et al.[1] also observed irreversible changes in the thickness of the crystalline domains that are, we believe, manifestations of the phenomenon of isothermal crystal thickening and therefore are not predicted by the present model.

In this paper we content ourselves with classical rubber elasticity theory,[15] in part because too little is known about the structure of the entangled network forming the amorphous domains to model the rubber elasticity forces with any additional detail. We discuss what we believe are the structural differences between the amorphous domains of semicrystalline polymers and the bulk melt, and we attempt to explain why the infrared and Raman experiments mentioned above are insensitive to the difference. We proceed by writing an expression for the total free energy of the system that includes terms for the rubber elasticity deformation of the amorphous domains and minimize that expression with respect to the number of monomers in the amorphous domain. A similar approach has already been considered by Fischer[16] and by Zachmann.[17] The primary difference in the present model is in the treatment of the entropy of the amorphous domains: We assume the entropy of the amorphous domains is affected, first, by the presence of entanglements that remain permanently in the system since (at least in the large molecular weight limit) disentanglement is impeded by the crystallites and second, by the presence of anisotropy in the amorphous domains and that both these effects can be modeled by standard rubber elasticity theory.

Equilibrium Properties of the Model

Any unperturbed polymer chain with both ends pinned exhibits a force of rubber elasticity tending to draw the ends of the chain together. The force, being entropic in nature, arises from thermal fluctuations of the chain. In a bead–spring model the force on one end is given by the extension of the last spring and is therefore directed along the instantaneous contour of the chain. (See Figure 1a.) In semicrystalline polymers, therefore, the force is directed into the amorphous domain tending to pull chains out of the crystal. (See Figure 1b.) Opposing this force is the thermodynamic tendency for the melt to crystallize.

Assume for the moment that chain transport between the two phases is impossible. The rubber elasticity forces shown in Figure 1b would be distributed evenly over the two planes, tending to draw the two planes together. This would, of course, be opposed by the incompressibility of

0024-9297/87/2220-1384$01.50/0

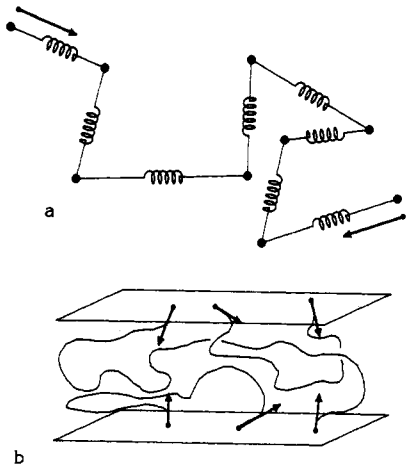

Figure 1. Diagram of the nature of the force of rubber elasticity. (a) In a bead–spring model, the force on the end of a chain pinned at both ends is seen to be directed instantaneously along the chain contour. (b) This means that a rubber elasticity force is present in semicrystalline polymers, tending to pull chains out of the crystal.

the amorphous phase. A balance between rubber elasticity forces and incompressibility exists in a bulk rubber, which is isotropic at equilibrium. Therefore, we might surmise that the amorphous domain would be isotropic. But of course, a bulk rubber is not expected to be isotropic near its surface, and so important departures from isotropy would be observed in the thin amorphous domains. In any case, in the absence of chain transport, the balance between rubber elasticity and incompressibility plays a major role in determining the amorphous structure.

Another thing happens when we permit transport. Assume equal densities of the two phases. When transport is possible, incompressibility is not important because the volume of the two phases can adjust as monomers move from one phase to the next. Therefore, the structure of the amorphous domains is expected to be dictated by a balance between rubber elasticity forces and the thermodynamic driving force toward crystallization.

In this model we assume an initially isotropic structure without transport between the phases and ask what changes develop when suddenly transport is allowed. We use a set of slip-links to model the effect of entanglements in the melt. We assume initially that there are N_0 backbone bonds in the portion of each chain lying between two slip-links. The slip-links play a role similar to that of cross-links in classical rubber elasticity: namely they represent pinning sites for the two ends of a chain of N_0 bonds. The value of N_0 cannot be specified precisely, but a value in the vicinity of the critical molecular weight for entanglements in the bulk melt, about 290 in polyethylene,[18] might be expected. In what follows we will usually let "chain" refer to the portion of a molecule between two slip-links. We assume that there are ν such chains in the amorphous phase, and therefore $\nu N_0 = N_m{}^0$ bonds in the melt initially. We then permit bonds to move between the two phases and examine the final state of the system when equilibrium is achieved between rubber elasticity forces and crystallization forces. During the approach to equilibrium, while bonds leave one phase and enter the other, we assume that chains in the melt are free to reptate through the slip-links. At equilibrium, we assume that each chain contains N bonds, with $N \neq N_0$. The number of chains, ν, remains constant, so that the melt at equilibrium contains $\nu N = N_m$ bonds. We assume that the volume of each amorphous domain adjusts via an affine deformation in the direction normal to the lamellar plane,

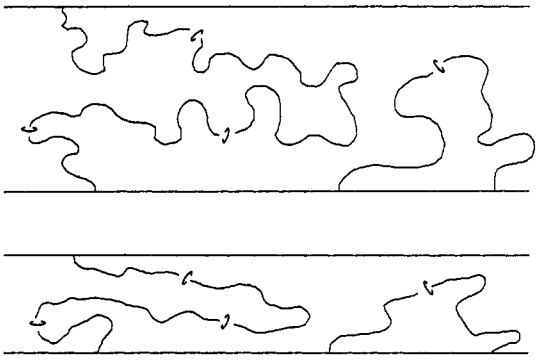

Figure 2. Schematic diagram of the affine transformation considered in this model. The original, isotropic domain of thickness H (above) is transformed affinely into an anisotropic domain of thickness $(N/N_0)H$ (below). Slip-links move in response to the affine transformation, and the number of bonds between slip-links change from N_0 to N to preserve the density of the domain.

with the slip-links moving accordingly, as depicted in Figure 2. The volume changes by a factor N/N_0, and no distortion in the lateral directions is assumed.

Classical rubber elasticity theory predicts that the free energy per chain of an ensemble of chains each having N bonds and following some end-to-end vector distribution characterized by a second moment $\langle R^2 \rangle$ is[15]

$$\frac{3}{2Na^2\beta}\langle R^2 \rangle \tag{1}$$

where a is the equivalent segment length and β is $(k_B T)^{-1}$ for k_B Boltzmann's constant and T the absolute temperature. Note the N dependence of eq 1. An ideal chain of length N pinned at both ends can decrease its free energy by adding monomers. This fact is of no importance in traditional rubber elasticity, where cross-links are chemical attachments, but is very important here since we are allowing the number of bonds per chain to change. The initial state of our model is characterized by $N = N_0$ and $\langle R^2 \rangle = N_0 a^2$, so we estimate the initial free energy per chain to be

$$G_i = 3/(2\beta) \tag{2}$$

Then the initial free energy per bond is

$$g_i = 3/(2N_0\beta) \tag{3}$$

For the final state of the chain we write

$$\langle R^2 \rangle_f = \langle x^2 \rangle_f + \langle y^2 \rangle_f + \langle z^2 \rangle_f \tag{4}$$

where

$$\langle x^2 \rangle_f = \langle y^2 \rangle_f = \frac{N_0 a^2}{3}; \qquad \langle z^2 \rangle_f = \frac{N_0 a^2}{3}\left(\frac{N}{N_0}\right)^2 \tag{5}$$

since the effect of the affine transformation as we have defined it is $\langle x^2 \rangle_f = \langle x^2 \rangle_i$, $\langle y^2 \rangle_f = \langle y^2 \rangle_i$, and $\langle z^2 \rangle_f = (N/N_0)^2 \langle z^2 \rangle_i$. Therefore, the final free energy per chain is

$$G_f = \frac{N_0}{2\beta N}\left(2 + \frac{N^2}{N_0{}^2}\right) \tag{6}$$

and the final free energy per bond is

$$g_f = \frac{N_0}{2\beta N^2}\left(2 + \frac{N^2}{N_0{}^2}\right) \tag{7}$$

The free energy difference per bond due to rubber elasticity is

$$\Delta g_r = g_f - g_i = \frac{1}{\beta}\left(\frac{N_0}{N^2} - \frac{1}{N_0}\right) \quad (8)$$

Note that this vanishes at $N = N_0$ as expected.

As stated above, we assume that initially there are N_m^0 and N_c^0 bonds in the amorphous and crystalline phases, respectively, and that after equilibrium is achieved, there are N_m and N_c, respectively, with $N_m^0 + N_c^0 = N_m + N_c$. Let ΔG represent the free energy of the two-phase system relative to the bulk melt, and let g_m and g_c represent the free energy per bond of the bulk melt and bulk crystal, respectively. Then we represent ΔG as the following:

$$\Delta G = N_m g_m + N_c g_c + N_m \Delta g_r + Q - (N_m^0 + N_c^0) g_m \quad (9)$$

In the above, the first three terms give the free energy of the two phases, Q represents the surface free energy term contributed by the interfacial planes, and the last term is the free energy of the bulk melt. We assume that Q is a constant, since during the transformation shown in Figure 2, the surface area of the interfacial plane does not change. Equation 9 becomes

$$\Delta G = N_c g_c - N_c g_m + Q + N_m \Delta g_r \quad (10)$$

Equilibrium is achieved when the derivative of ΔG with respect to N_m vanishes

$$0 = -g_c + g_m + \Delta g_r + N_m \frac{\partial \Delta g_r}{\partial N_m} \quad (11)$$

We proceed by differentiating eq 8, remembering that $N_m = \nu N$. Equation 11 becomes

$$g_c = g_m - \frac{1}{\beta}\left(\frac{N_0}{N^2} + \frac{1}{N_0}\right) \quad (12)$$

which we recognize as a matching of the chemical potentials of the two phases. The solution of eq 12 for N is

$$N = N_0(N_0\beta\Delta g - 1)^{-1/2} \quad (13)$$

where $\Delta g = g_m - g_c$ is the free energy difference per bond between the two bulk phases. We previously assumed that N is proportional to N_m, the number of bonds in the amorphous phase. This is equivalent to assuming a proportionality between N and the average thickness of the amorphous layers. Therefore, we write

$$N = \gamma d;\ N_0 = \gamma d_0 \quad (14)$$

for d_0 and d the initial and final thicknesses of the amorphous domains and obtain

$$d = d_0(N_0\beta\Delta g - 1)^{-1/2} \quad (15)$$

Equation 15 indicates that the thickness of the amorphous domain depends on temperature through the temperature dependence of $\beta\Delta g$. We may also write

$$d^{-2} = d_0^{-2}(N_0\beta\Delta g - 1) \quad (16)$$

predicting a linear relationship between d^{-2} and $\beta\Delta g$.

In the following, we employ the approximation

$$\Delta g = \frac{\Delta h_f \Delta T}{T_m} \quad (17)$$

for Δh_f the heat of fusion per bond, T_m the equilibrium melting temperature, and $\Delta T = T_m - T$, the undercooling. This approximation is valid for small values of ΔT. Using values appropriate for polyethylene ($\Delta h_g = 2.80 \times 10^9$ erg/cm^3, $T_m = 418.7$ K)[19] yields

$$\beta\Delta g = 1.1(\Delta T/T) \quad (18)$$

Two separate least-squares fits, one to eq 15 and one to eq 16, were applied to each set of data points obtained by Tanabe et al.[1] for samples crystallized at a given temperature. Figures 3–5 display fits of the data of Tanabe et al.[1] for d to eq 16, while Figures 6–8 display fits of eq 15. The large deviations from linearity in Figures 3–5 at large Δg values are to be expected since at such temperatures eq 18 is invalid.[20] Because of this, experimental data at temperatures $T \geq 100$ °C only were used for fitting. The values of N_0 and d_0 obtained in each of the fits are shown in Table I. The best fit values of N_0 tend to be smaller than the above estimation of $N_0 = 290$. However, it should be noted that a fairly wide range of N_0 and d_0 values can be chosen to fit the data. The slopes of the lines in Figures 3–5 can be determined with a fair degree of accuracy, but, as is obvious from eq 16, this only fixes the value of N_0/d_0^2.

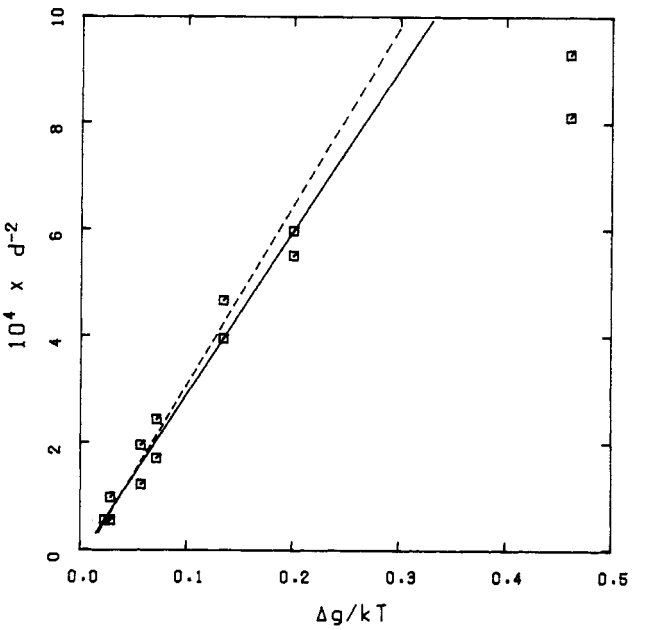

Figure 3. Plot of the Tanabe–Strobl–Fischer data,[1] for samples crystallized at 125 °C, plotted as d^{-2} vs. $\beta\Delta g$, for d the amorphous domain thickness and Δg the free energy difference per bond between the two bulk phases. The solid line is obtained by a least-squares fit to eq 15, the dashed line by a linear least-squares fit to eq 16.

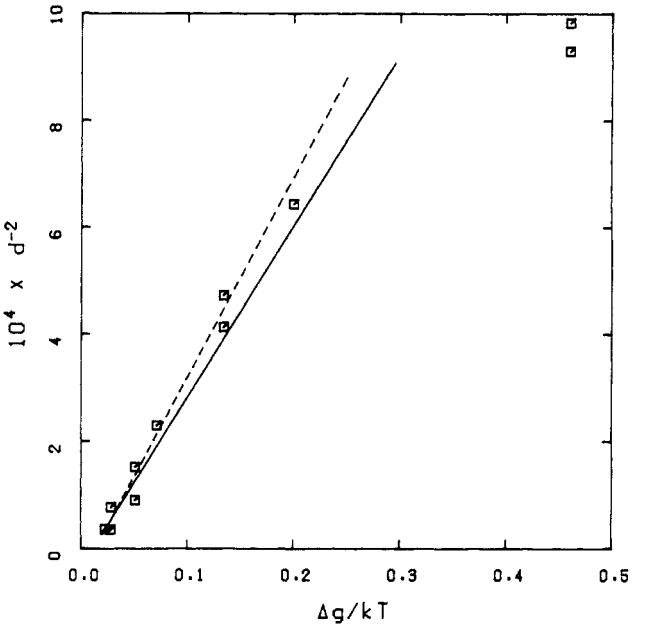

Figure 4. Same as Figure 3, but for a crystallization temperature of 127 °C.

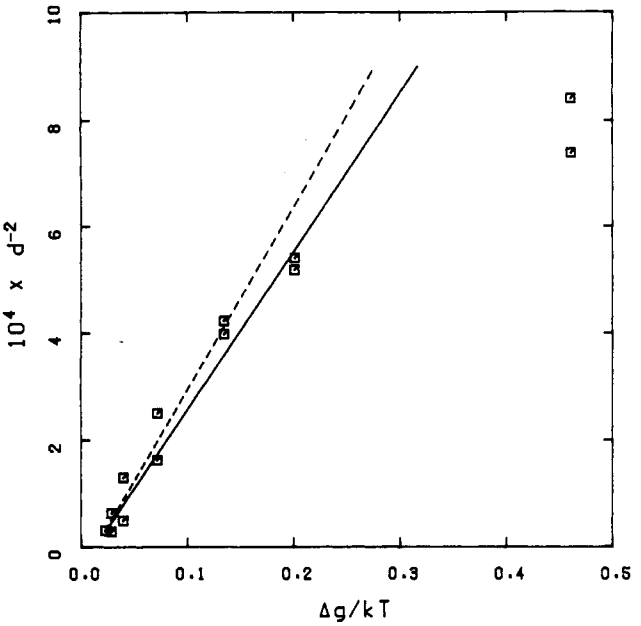

Figure 5. Same as Figure 3, but for a crystallization temperature of 131 °C.

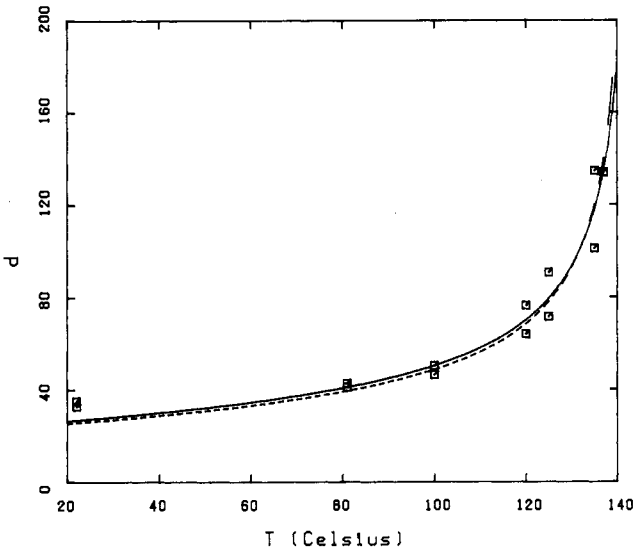

Figure 6. Plot of the Tanabe–Strobl–Fischer data,[1] for samples crystallized at 125 °C, with the amorphous domain thickness plotted as a function of temperature according to eq 15. The solid curve is obtained by a least-squares fit to eq 15, the dashed curve by a linear least-squares fit to eq 16.

Table I
Best Fit Values of N_0 and d_0 Obtained from the Tanabe–Strobl–Fischer[1] Data

T_x[a]	data fit to eq	N_0	d_0, Å
125	15	208	261
	16	130	197
127	15	83	161
	16	70	137
131	15	75	159
	16	72	145

[a] Crystallization temperature.

To obtain a value of either N_0 or d_0 separately, we must use the intercept. But since the lines in Figures 3–5 nearly intercept the origin, the intercept cannot be determined too precisely. Therefore, a rather broad set of N_0 and d_0 values, chosen such that N_0/d_0^2 is constant, successfully fits the data. The best fit values of N_0 and d_0 tend to decrease with increasing crystallization temperature.

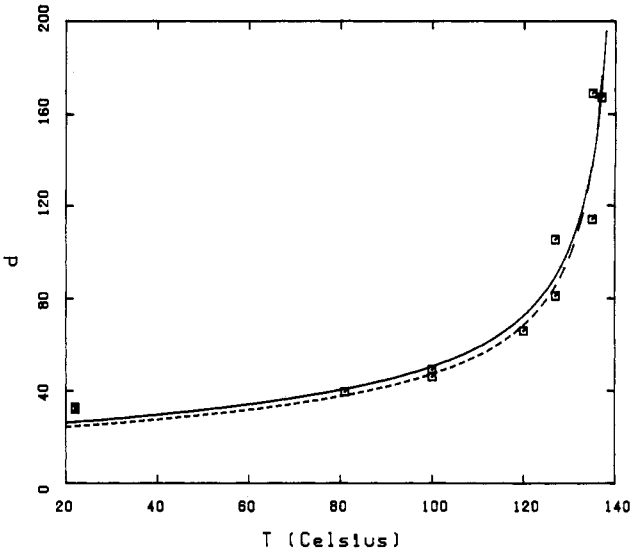

Figure 7. Same as Figure 6, but for a crystallization temperature of 127 °C.

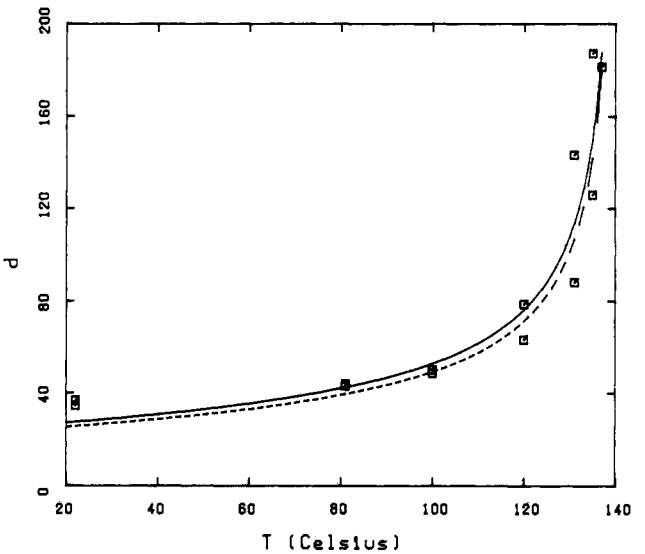

Figure 8. Same as Figure 6, but for a crystallization temperature of 131 °C.

These results predict large changes in both the anisotropy and thickness of the amorphous layers with temperature.

Note that d is undefined whenever $N_0\beta\Delta g < 1$. This means that for undercoolings below some critical value ΔT_c the two-phase equilibrium cannot be achieved, where

$$\Delta T_c = T_m(1.1N_0 + 1)^{-1} \quad (19)$$

Since best fit N_0 values lie over a large range, precise values of ΔT_c are not known. The N_0 values in Table I predict that ΔT_c is on the order of 2–5 K. The driving force for crystallization is proportional to the undercooling, so that at small undercoolings the rubber elasticity force dominates and is strong enough to pull the crystals apart. ΔT_c corresponds to the temperature at which eq 15 diverges or eq 16 equals zero.

Kinetic Properties of the Model

In this section, we estimate the amount of time required for the equilibrium state calculated in the last section to be achieved. We assume that the mechanism permitting transport between the two phases is a coupled twist–translation of the entire polymer stem produced by the passage of a soliton along the stem.[3-11] This mechanism has already been proposed for the crystalline α relaxation

and accounts very well for the observed properties of the relaxation. The net effect of the passage of the soliton in any particular polymer crystal is to advance the helical stem up or down by one repeat unit with a combined twist and translation. For example, in polyethylene a 180° rotation combined with a $c/2$ translation (for c the unit cell dimension along the stem axis) is produced. A sequence of such moves produces a net reptation of the polymer stem within the crystal.

From the above we have

$$\frac{\partial \Delta G}{\partial N_m} = \beta^{-1}(1.1\Delta T/T - N_0^{-1} - N_0/N^{-2}) \qquad (20)$$

which is, of course, the amount by which ΔG increases when a bond leaves the crystal and enters the amorphous domain. Therefore, we estimate the rate at which N_m changes with time as

$$\frac{\partial N_m}{\partial t} = \tau k_\alpha N_s \left[\exp\left(-1.1\frac{\Delta T}{T} + \frac{N_0}{N^2} + \frac{1}{N_0} \right) - 1 \right] \qquad (21)$$

where k_α is the rate at which solitons pass through the crystalline stem. N_s is the number of crystalline stems, and τ is the fraction of stem reptations that transfers bonds to or from the amorphous domain. The exact value of τ is unknown, but we expect it to be on the order of $^1/_3$, which is the fraction of random reentry predicted by the gambler's ruin model,[21-24] times a factor of about $^1/_2$, which is explained below. In any case, we assume that τ is within an order of magnitude of unity. Equation 21 represents the difference between bonds leaving the melt at a rate

$$\tau k_\alpha N_s$$

and bonds entering the melt at a rate

$$\tau k_\alpha N_s \exp\left(-1.1\frac{\Delta T}{T} + \frac{N_0}{N^2} + \frac{1}{N_0} \right)$$

By including the proportionality constant τ, we make explicit the realization that not every crystalline stem that reptates up or down in the crystal carries a bond from one phase to another. Some reptation motions carry bonds from the melt into a tight fold, but since the motion also requires rotation of the stem, the tight fold must accept a 180° twist. Since many crystalline stems terminate in tight folds, an effective mechanism for the distribution of bonds between stems with tight folds and stems with random reentrant folds is necessary if the rate at which bonds change phase is not to be limited by the passage of a bond, with its accompanying twist, through a tight fold. It could conceivably require either a great deal of time or of energy for a 180° twist to work its way through a tight fold, probably requiring a number of bond rotational transitions. However, we do not believe that the problem is so severe for polyethylene. Since polyethylene is not tactic, its twists are enantiomeric.[25] Twists of either handedness occur with equal energy. If first a right-handed and then a left-handed twist, or vice versa, is sent from a random reentrant fold through a stem into a tight fold, the net effect would be to send two bonds and no twist into the tight fold, which could then presumably be rapidly distributed among the two stems attached to the tight fold, with the net effect of carrying two bonds from the melt into two adjacent crystalline stems. A metastable transition state, consisting of a tight fold holding one extra bond and a 180° twist, would exist until the second twist arrived. Such a metastable fold would probably reject a second twist of the wrong handedness, which would then have to work its way back out. A tight fold at one end of a stem could send two bonds to a tight fold at the other end by first sending a twist of given handedness to the other fold and then by sending a second twist of opposite handedness. Between the passage of the first and second twist, both folds would find themselves in a metastable state. These concepts are displayed schematically in Figure 9. Diagrams a–e (the top row of Figure 9) show how bonds can pass from the melt through a tight fold and diagrams f–j show how bonds can pass from one tight fold to another. In diagrams a–c, we see the passage of a right-handed soliton (+) from the melt into a tight fold. The soliton is indicated schematically by the bump in the chain in diagram b and carries +180° of twist and an additional bond. In diagram c, the tight fold must accept both the twist and the additional bond, creating a metastable fold indicated schematically by the angular fold labeled (+). In diagram d we see the passage of a left-handed soliton (–) carrying –180° of twist and an additional bond. The negative twist of the second soliton cancels the positive twist in the metastable fold to create a new fold, with the two extra bonds distributed between the two stems, as shown in diagram e. The net effect has been the transport of two bonds from the melt into the crystal. In diagram g we see the passage of a right-handed soliton that has been emitted by a tight fold. Before the soliton is emitted, or as the soliton leaves, the two stems to which the fold is attached each shorten by one bond and then the soliton carries away one bond and +180° of twist, leaving behind a metastable fold of the same type as in diagram c but holding –180° of twist. When the right-handed soliton arrives in the second tight fold, a second metastable fold is created. Then in diagram i, the first metastable fold emits a left-handed soliton and becomes a regular fold, and the left-handed soliton couples with the second metastable fold in diagram j to form another regular fold. The net effect has been the transport of two bonds between different crystalline stems joined by tight folds. The requirement that only one twist in two would be accepted is accommodated by introducing a factor of $^1/_2$ into the parameter τ. Polymers with tacticity only admit solitons of a given handedness determined by the handedness of the helix,[11] just as a screw can only turn one way. Therefore, an equation such as eq 21 is probably not applicable to any polymer with tacticity, and the present kinetic arguments probably would not apply. Clearly, they also would not apply to any polymer not exhibiting the α relaxation.

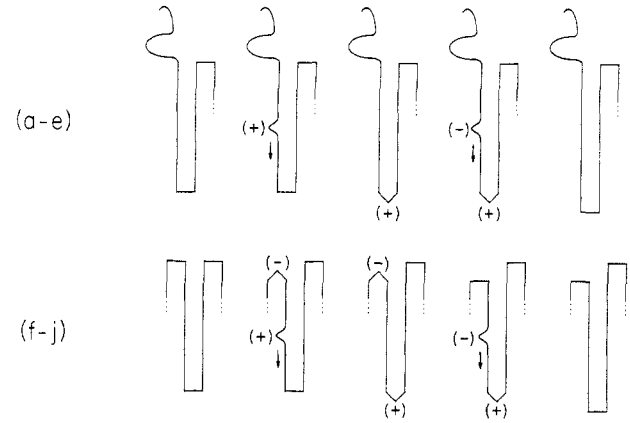

Figure 9. Schematic diagram of a possible mechanism by which the α relaxation permits stem length changes in polyethylene crystals without the necessity of working chain twist through tight folds.

In writing eq 21 we are also assuming that reptation in the amorphous domain occurs much more rapidly than

reptation within the crystal. This assumption is justified empirically by our current understanding of the mechanical and dielectric α relaxations and therefore appears valid at least in the temperature range over which the α relaxation is usually observed. As explained by Boyd,[9,10] the dielectric relaxation occurs in the crystal, while the mechanical relaxation occurs in the amorphous domain, although requiring the presence of the crystal. Reptation in the crystal is not itself mechanically active but frees up the amorphous domain so it can relax. Since the observed activation energies for the mechanical and dielectric processes are comparable, we conclude that reptation in the crystal is the rate-determining step. Therefore, at least at temperatures where the α relaxation is observed (above perhaps 70 °C in polyethylene), we are justified in neglecting amorphous domain reptation in eq 21.

According to Mansfield and Boyd,[4] the following holds for the rate of soliton passage in the polyethylene crystal:

$$k_\alpha = (k_B T/h)F(n_c) \exp(-\Delta G^\ddagger/k_B T) \quad (22)$$

where h is Planck's constant and $\Delta G^\ddagger$ is the activation free energy which can be approximated as

$$\Delta G^\ddagger = 18.1 \text{ kcal mol}^{-1} - (0.01 \text{ kcal mol}^{-1} \text{ K}^{-1})T \quad (23)$$

and where

$$F(n_c) = [Pn_c + (1 + P^2 n_c^2)^{1/2}]^{-1} \quad (24)$$

represents a stem-length-dependent soliton scattering contribution, where n_c is the number of bonds per stem and P is a fitting parameter yielding good agreement when $P = 10^{-2}$. The following expression gives n_c in terms of the other parameters appearing above:

$$n_c = n_c^0 + (\nu/N_s)(N - N_0) \quad (25)$$

Equation 21 becomes

$$\frac{\delta N}{\delta t} = \left(\frac{\tau N_s}{\nu}\right)\left(\frac{k_B T}{h}\right) \exp\left(\frac{-\Delta G^\ddagger}{k_B T}\right) F(n_c) \times \left[\exp\left(-1.1\frac{\Delta T}{T} + \frac{N_0}{N^2} + \frac{1}{N_0}\right) - 1\right] \quad (26)$$

with $F(n_c)$ as given by eq 24 and 25. In all cases of interest, the ratio N_s/ν is expected to be of order of magnitude of unity. Therefore we proceed by setting the quantity $\tau N_s/\nu = 1$. In addition, $F(n_c)$ is within an order of magnitude of 1 for all values of n_c of interest, so to avoid the necessity of considering dependence on terms such as n_c^0 appearing in eq 25, we set $F(n_c) = 1$. Both of these assumptions only permit an order of magnitude estimation of the time scale.

Equation 26 was integrated numerically, with the results for $N_0 = 290$ shown in Figure 10. This calculation indicates that equilibration is possible in 1 s or less at many values of the undercooling. At room temperature (assuming eq 17 is valid at such temperatures) we predict equilibration in less than a minute, although as pointed out above, our empirical justification for neglecting amorphous domain reptation is not so strong at such temperatures.

Consequences for the Predictions of the Gambler's Ruin Model

Guttmann, DiMarzio, and Hoffman have developed the gambler's ruin model of the amorphous domains of semicrystalline polymers.[21,22] This model treats individual chains in the amorphous domains as random walks between two absorbing barriers and permits predictions about quantities such as the degree of adjacent vs. random reentry, the fraction of tie chains (i.e., chains in the amorphous domain that bridge two crystallites), or the radius of gyration of individual polymer molecules.[26,27] The model predicts that these quantities depend on both the thickness and the chain anisotropy of the amorphous domains. This is important to the arguments in this paper, since we predict changes in both the thickness and the anisotropy. The amount of time required for equilibration calculated above would be much greater if gambler's ruin constraints required changes in the radius of gyration, the number of tie molecules, or the nature of chain folding. Fortunately, since the domain thickness and anisotropy are both proportional to N/N_0, their combined effects are compensatory. This fact is established in the Appendix. The structural changes discussed in the above sections occur without gross reorganization of individual chains. Quantities such as the radius of gyration, the number of tie chains, or the amount of adjacent vs. random reentry do not change as the amorphous domains change their structure with temperature.

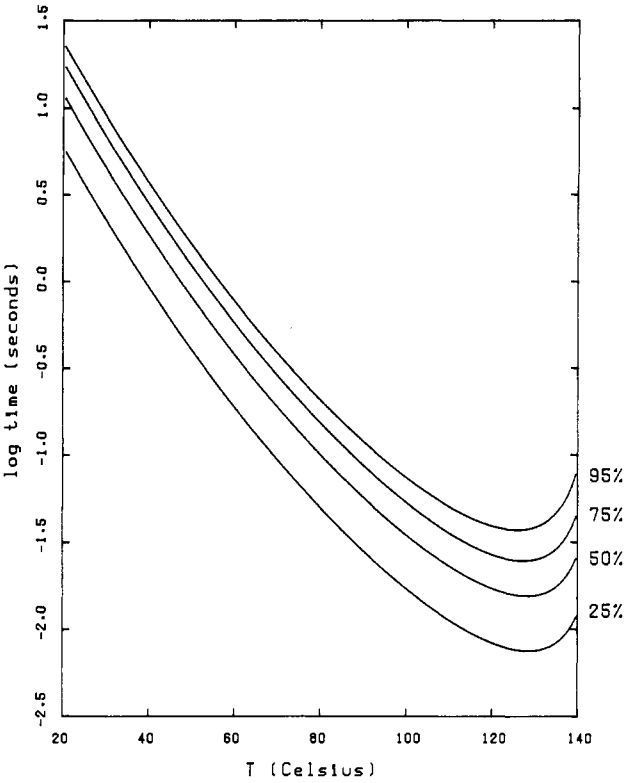

Figure 10. This diagram displays the amount of time at any given undercooling as predicted by solutions to eq 26 for N to change from N_0 to within 25%, 50%, 75%, or 95% of its equilibrium value.

Invariance of the Local Structure

As was stated in the Introduction, a number of experiments have been performed that do not detect structural differences between the bulk melt and the amorphous domains of semicrystalline polymers.[2] We believe that this is because such experiments (e.g., Raman or IR vibrational spectra) examine local structure and dynamics and are relatively insensitive to rubber elasticity deformations, which more strongly affect global properties.

In support of this argument, we present the following calculation. We compute the probabilities that two successive steps in a six-choice random walk of N steps on the simple cubic lattice are either parallel or antiparallel when the end-to-end vector of the walk is required to obey this distribution function

$$P(x,y,z) = BC^{1/2}\pi^{-3/2} \exp(-Bx^2 - By^2 - Cz^2) \quad (27)$$

with $B = {}^1/_{20}$ and $C = 45/N^2$. Equation 27 has moments given by eq 5 with $N_0 = 30$. Therefore, when $N = 30$ it approximates the exact distribution of 30-bond walks, and for values of N different from 30, it yields the anisotropic distribution of eq 5. The calculation is performed by the following enumeration procedure. Consider a particular lattice site (x,y,z), where x, y, and z are integers. We also restrict ourselves to even N, which implies that the sum $x + y + z$ is even. We assume that during the walk we take n_1 steps in the $+x$ direction, n_2 in the $-x$ direction, n_3 in the $+y$ direction, n_4 in the $-y$ direction, n_5 in the $+z$ direction, and n_6 in the $-z$ direction. We must consider all possible values of n_1, n_2, etc., but the following conditions imply that only two of the six values can be chosen independently:

$$n_1 + n_2 + n_3 + n_4 + n_5 + n_6 = N \tag{28a}$$

$$n_1 - n_2 = x \tag{28b}$$

$$n_3 - n_4 = y \tag{28c}$$

$$n_5 - n_6 = z \tag{28d}$$

The additional requirement that n_1, n_2, etc., are all nonnegative further restricts the number of possibilities. The number of unique walks to the lattice site (x,y,z) with given values of $(n_1,n_2,n_3,n_4,n_5,n_6)$ is

$$N![n_1!n_2!n_3!n_4!n_5!n_6!]^{-1} \tag{29}$$

The probability that bond i is in the $+x$ direction within the ensemble of fixed $(n_1,n_2,n_3,n_4,n_5,n_6)$ values is n_1/N. The probability that bond i and $i + 1$ are simultaneously in the $+x$ direction then is $(n_1/N)[(n_1 - 1)/(N - 1)]$. It follows that the probability that bond i and bond $i + 1$ are simultaneously parallel is

$$[N(N-1)]^{-1} \sum_{j=1}^{6} n_j(n_j - 1) \tag{30}$$

The probability that bonds i and $i + 1$ are simultaneously in the directions $+x$ and $-x$, respectively, is $(n_1/N)[n_2/(N - 1)]$. The probability that bonds i and $i + 1$ are simultaneously antiparallel is, it follows

$$2[N(N-1)]^{-1}(n_1n_2 + n_3n_4 + n_5n_6) \tag{31}$$

Equations 30 and 31 actually give the probabilities for any pair of steps in the walk. It is not necessary that the two steps be consecutive. Equations 30 and 31 represent the probabilities that two steps are parallel or antiparallel, respectively, within an ensemble for which both (x,y,z) and $(n_1,n_2,n_3,n_4,n_5,n_6)$ are fixed. Therefore, we obtain averages for an ensemble in which only (x,y,z) is fixed by averaging over all allowed values of $(n_1,n_2,n_3,n_4,n_5,n_6)$ consistent with the given value of (x,y,z) with each contribution weighted according to eq 29. Then we average over all possible values of (x,y,z) consistent with a given value of N, weighting each contribution according to eq 27. The result is the probability that two successive steps are either parallel or antiparallel when a particular anisotropic, harmonic force is applied to the ends of the chain. These sums were evaluated directly, which is possible in not too long a time if N is not too large. The results are shown in Figure 11. The probabilities remain very near ${}^1/_6$ until rather large distortions of the end-to-end distribution function are applied. This indicates that rather large forces can be applied to the ends of a chain with only modest distortion of the local chain structure. This would imply only modest changes in the trans–gauche population of polyethylene during transformation, and it does not seem too surprising that IR or Raman spectral experiments do not detect structural differences. This is also consistent with classical rubber elasticity theory, which holds that enthalpic contributions to the free energy during elastic deformation are negligible. Presumably, any large change in local structure would change the internal energy.

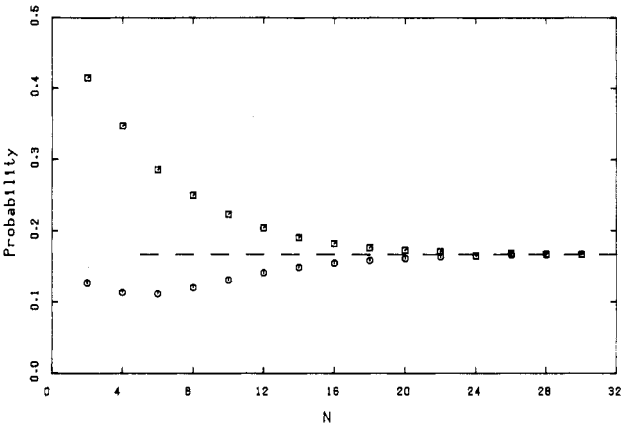

Figure 11. Probability of finding two successive steps of a six-choice walk of length N on the simple cubic lattice in either a parallel or an antiparallel arrangement when the end-to-end vector is forced to follow a distribution of the form of eq 27. The upper set of points corresponds to a parallel arrangement, the lower set to an antiparallel arrangement. The horizontal dashed curve displays the limiting value of ${}^1/_6$.

Discussion and Conclusions

As discussed above, the best fit values of N_0 and d_0 shown in Table I are subject to some uncertainty, the ratio N_0/d_0^2 only being well characterizable from the data. However, if we assume that the trend in d_0 as a function of crystallization temperature is not artificial, some speculation is possible. We have assumed that the initial state of the amorphous domain, as characterized by the quantities d_0 and N_0, is isotropic. There is no particularly good reason for this assumption, since anisotropy might be present initially. This obscures any physical meaning that one might attach to be best fit values of d_0 and N_0 in Table I. One could argue that d_0 does not correspond to the initial thickness of the domain immediately following solidification but to that particular thickness at which the domain becomes isotropic. In addition, we have no particular explanation for why the best fit N_0 values are less than the entanglement length of the bulk melt, except that this might indicate that entanglements become concentrated in the amorphous domains during solidification. In any case, the Tanabe–Strobl–Fischer[1] measurements indicate dependence upon crystallization temperature, so it seems reasonable that d_0 and N_0 characterize the initial state of the amorphous domain.

This model assumes that the sum of the thicknesses of the two domains is constant, with one always growing at the expense of the other. It also assumes that both thicknesses change reversibly, with recovery of initial values after a heating–cooling cycle. The crystallites were observed by Tanabe et al.[1] to decrease in thickness during heating while the amorphous domains thickened, but only the amorphous domains recovered their initial thickness upon recooling. After completion of the cycle, the crystallites invariably were thicker. However, this is not surprising since it is well-known that polymer crystals thicken isothermally.[12,13] Superimposed on the process described here is the well-known phenomenon of isothermal crystal thickening. The fact that the amorphous domains return to their initial thickness after recooling indicates that during an isothermal thickening experiment the thickness of the amorphous domains would not change. The amorphous domain thickness is determined by the

temperature and the previous history of the domain but not by the crystal thickness. It is believed that the driving force for isothermal crystal thickening is the term Q in eq 10. That term is proportional to the interfacial area, which must decrease if the crystals thicken without an amorphous domain thinning. As discussed above and in the Appendix, the changes described in this paper preserve the folding structure, the radius of gyration, and the interfacial area, and the invariance of these global properties accounts for the relative speed of the kinetics. This leads to the speculation that the slower phenomenon of isothermal crystal thickening is a process involving global rearrangement of the folding structure, the radius of gyration (probably including the anisotropy of its major and minor components), and of course the interfacial area.

The precise transition temperature of polyethylene has been a subject of controversy.[28] In our analysis we have employed the value 418.7 K, although some authors prefer a value several degrees lower. We are able to obtain adequate fits to the Tanabe–Strobl–Fischer data using 414.2 K as well. We do not intend in this paper to support either value, but it is possible to speculate that the melting point depression brought on by the ΔT_c effect discussed above might contribute to the confusion.

In this paper we have made assumptions specific to polyethylene, namely the existence of an α relaxation occurring via an enantiomeric soliton. As discussed above, these properties are expected to enhance the transport rate between the two phases. In general, we expect longer equilibration times in most other polymers. Any semicrystalline polymer is expected to have rubber elasticity forces arising in the amorphous domains, but there may be cases in which transport is so slow that rubber elasticity forces are balanced by incompressibility, and the effects described here would not be seen.

This model inherits all the shortcomings of classical rubber elasticity theory,[15] for example, in the assumption that pinning sites for the ends of the chain move affinely and in the Gaussian assumption embodied in eq 1. However, the major conclusion, that a balance between rubber elasticity and crystallization forces produces temperature-dependent changes in the structure of the amorphous domains, is based on fundamental thermodynamic arguments and the empirical realization that transport occurs between the two phases.

Appendix: A Continuum Gambler's Ruin Model

The gambler's ruin model, as developed by Guttman, DiMarzio, and Hoffman,[21,22] treats the structure of chains in the amorphous domains of semicrystalline polymers. It is based on the statistics of random walks between two absorbing barriers. A number of treatments, using different sorts of random walks, have been given.[21-24] The physically significant results of the model are independent of the detailed nature of the walk. For our purposes, we have found a continuum random walk, based on the diffusion equation, to be most appropriate, and so in this appendix we develop the gambler's ruin model from such walks. This permits us to demonstrate the lack of gross reorganization as discussed above.

We consider random walks between the two absorbing planes $z = 0$ and $z = L$. We let $W(x,y,z,t)$ be the probability density that the walk is at the point (x,y,z) after t steps. (The unit of "time" in our case is the number of bonds.) The "time" development of W is given by the diffusion equation

$$\frac{\partial W}{\partial t} = D_1\frac{\partial^2 W}{\partial x^2} + D_1\frac{\partial^2 W}{\partial y^2} + D_2\frac{\partial^2 W}{\partial z^2} \qquad \text{(A1)}$$

As is well-known, the solution to eq A1 in the absence of absorbing or reflecting barriers is a Gaussian distribution when W at $t = 0$ is a dirac delta function. We obtain appropriate values of the "diffusion" coefficients by forcing that Gaussian distribution to have the moments given by eq 5. The moments expected from eq A1 are

$$\langle x^2\rangle = \langle y^2\rangle = 2D_1t; \qquad \langle z^2\rangle = 2D_2t \qquad \text{(A2)}$$

Comparing these with eq 5 yields

$$D_1 = \sigma^{-1}(a^2/6); \qquad D_2 = \sigma(a^2/6) \qquad \text{(A3)}$$

where we let σ represent the ratio N/N_0 and where we have set $t = N$. Therefore, σ characterizes the changes in both the thickness and the anisotropy. The special case of isotropic random walks is obtained by setting $\sigma = 1$.

The expression

$$W(x,y,z,t) = \sum_{j=1}^{\infty}\int d\kappa\, A_j(\kappa,t)e^{i\kappa\cdot\mathbf{r}}\sin\left(\frac{\pi jz}{L}\right) \qquad \text{(A4)}$$

represents the most general Fourier development of the function W having the boundary conditions $W(z=0) = W(z=L) = 0$, which is appropriate for absorption at the two planes. We let $\mathbf{r}$ represent the two-vector (x,y) and κ its reciprocal-space conjugate. We assume that the walks begin at the site $(x,y,z) = (0,0,s)$ and proceed until they are absorbed at one of the two faces. We assume that the value of s is arbitrary but require $s \ll L$. We also require s to change with the affine deformation so that it too is proportional to σ. Therefore

$$W(x,y,z,0) = \delta(x)\delta(y)\delta(z-s) \qquad \text{(A5)}$$

for δ the dirac delta function. This implies that

$$A_j(\kappa,0) = (2\pi^2L)^{-1}\sin(\pi js/L) \qquad \text{(A6)}$$

The diffusion equation implies

$$A_j(\kappa,t) = A_j(\kappa,0)\exp[-(D_1\kappa^2 + D_2(\pi j/L)^2)t] \qquad \text{(A7)}$$

Combining all the above yields

$$W(x,y,z,t) = (2\pi LD_1t)^{-1}e^{-r^2/4D_1t}\sum_{j=1}^{\infty}\sin(\pi js/L)\sin\left(\frac{\pi jz}{L}\right)e^{-D_2t\pi^2j^2/L^2} \qquad \text{(A8)}$$

Now define

$$W'(z,t) = \int d\mathbf{r}\, W(x,y,z,t) = (2/L)\sum_{j=1}^{\infty}\sin(\pi js/L)\sin\left(\frac{\pi jz}{L}\right)e^{-D_2t\pi^2j^2/L^2} \qquad \text{(A9)}$$

representing the probability of finding the walk at z after t steps. Note that[29] $D_2[\partial W'/\partial z]_{z=0}\,dt$ and $-D_2[\partial W'/\partial z]_{z=L}\,dt$ are the fraction of chains being absorbed at $z = 0$ and $z = L$, respectively, in the "time" interval $(t, t + dt)$. Therefore

$$P(t) = D_2([\partial W'/\partial z]_{z=0} - [\partial W'/\partial z]_{z=L}) \qquad \text{(A10)}$$

$$= (4\pi D_2/L^2)\sum_{j\ \text{odd}} j\sin\left(\frac{\pi js}{L}\right)e^{-D_2t\pi^2j^2/L^2} \qquad \text{(A11)}$$

is the probability that a walk contains t bonds. The average number of bonds in a walk from the time that it is initiated at $t = 0$ until it is absorbed at one of the two faces is[30]

$$\langle t \rangle = \int_0^\infty dt\ tP(t) = \frac{s(L-s)}{2D_2} = \frac{sL}{2D_2} \qquad \text{(A12)}$$

with the latter equality holding in the limit $s \ll L$. Note that the average walk length is dependent on the arbitrary parameter s. This is an example of the "Vonk paradox",[23] which arose when it was recognized that the average walk length is dependent on details concerning the initiation of each walk. This result was considered paradoxical because the average walk length was expected to determine model predictions of universal qualities. The paradox was resolved when it was recognized that the average walk length is not a determining factor.[24] All the physically significant results given below are independent of s to leading order in s/L.

We proceed by assuming that a fraction ϕ of the crystalline stems present in the system are followed by random walks of average length $\langle t \rangle$ and that the remaining fraction $1 - \phi$ of the stems is followed by tight folds of effective length zero. The value of ϕ is then adjusted so that the amorphous domains have the correct density. Let N_s be the number of crystalline stems. Then the number of monomers in the crystal is $N_s l_c / l_m$ where l_c and l_m are the lengths of a crystalline stem and of a monomer within the crystal, respectively. The number of monomers in the amorphous domains is $\phi N_s \langle t \rangle$. The crystal density is proportional to N_s/l_m, while the amorphous density is proportional to $\phi N_s \langle t \rangle / L$. By combining all of the above, we obtain

$$\phi = 2D_2 \rho / l_m s \qquad \text{(A13)}$$

where ρ represents the ratio of amorphous to crystalline density. We note for later reference that the quantity ϕ is dependent on s but that the product ϕs is not. We assume that a fraction $1 - \phi$ of the crystalline stems is followed by "tight folds" returning to the crystallite with zero length, while the remaining fraction, ϕ, of stems is followed by chains following the random walk statistics outlined above. Of these chains, we refer to those returning to the $z = 0$ plane as amorphous loops and those crossing the amorphous domain to the $z = L$ plane as ties. Then the fraction of amorphous loops returning to the point $(x,y,0)$ in "time" interval $(t, t + dt)$ is given by

$$f_L(x,y,t)\ dt = \phi D_2 [\partial W / \partial z]_{z=0}\ dt \qquad \text{(A14)}$$

and the fraction of ties reaching the point (x,y,L) in the same interval is

$$f_T(x,y,t)\ dt = -\phi D_2 [\partial W / \partial z]_{z=L}\ dt \qquad \text{(A15)}$$

The total fraction of amorphous loops is obtained by integrating eq A15 over all possible values of x, y, and t. We obtain[30]

$$\int_{-\infty}^{\infty} dx \int_{-\infty}^{\infty} dy \int_0^\infty dt\ f_L(x,y,t) = \phi(1 - s/L) \qquad \text{(A16)}$$

Likewise, for the total fraction of ties, we obtain[30]

$$\int_{-\infty}^{\infty} dx \int_{-\infty}^{\infty} dy \int_0^\infty dt\ f_T(x,y,t) = \phi s/L = \delta \qquad \text{(A17)}$$

which we set equal to δ by definition. The "mean-square throw length" of an amorphous loop, i.e., the mean square distance between the points (0,0,0) and $(x,y,0)$ is[30]

$$\phi^{-1}(1 - s/L)^{-1} \int_{-\infty}^{\infty} dx \int_{-\infty}^{\infty} dy \int_0^\infty dt\ f_L(x,y,t)(x^2 + y^2) = (4/3)sL(D_1/D_2) \qquad \text{(A18)}$$

to leading order in s/L. Therefore, the mean-square throw length of any loop is

$$(4/3)s\phi L(D_1/D_2) \qquad \text{(A19)}$$

Likewise, the mean-square throw length of ties is[30]

$$(2/3)(D_1/D_2)L^2 \qquad \text{(A20)}$$

Each crystalline stem is followed with probability $1 - \phi$ by a tight fold, $\phi(1 - s/L)$ by an amorphous loop, and $\phi s/L$ by a tie. This seems to be in violation of our statement above that all physically significant quantities are independent of s. Likewise, the mean-square throw length of amorphous loops is s-dependent. However, when all loops are considered, both tight folds and amorphous loops, the mean-square throw length, eq A19, and the fraction of loops, $1 - \phi s/L$, are s-independent. The ensemble of all loops exhibits universal properties. It is only when we segregate the ensemble into tight folds and amorphous loops that s dependencies develop. This segregation is arbitrary for $s \ll L$, since then there are very many very short amorphous loops. This explains the resolution of the Vonk paradox;[23] for additional details, see ref 24.

In this paper, we are more concerned with how the above properties depend on the quantity σ. Remember that D_2, L, and s are all proportional to σ, while D_1 is proportional to σ^{-1}. It then becomes obvious that the physically significant quantities considered above are independent of σ, which is to say that they do not change when the thickness and anisotropy of the amorphous domains adjust to temperature changes.

The gambler's ruin model also permits prediction of the mean-square end-to-end vector and of the radius of gyration.[26,27] To compute these quantities, we divide the chain into a set of virtual bonds, each one comprising one crystalline stem and the amorphous run following it. The mean-square end-to-end distance is given by[26]

$$\langle R^2 \rangle = n[\langle V^2 \rangle + 2 \sum_{j=1}^{\infty} \langle V_0 \cdot V_j \rangle] \qquad \text{(A21)}$$

where n is the number of crystalline stems, $\langle V^2 \rangle$ is the mean-square length of one of the virtual bonds, and $\langle V_0 \cdot V_j \rangle$ is the mean projection of the j-th virtual bond on the zeroth. The quantities on the right are given by[26]

$$\langle V^2 \rangle = \epsilon \langle x^2 + y^2 + z^2 \rangle_{loop} + \delta \langle x^2 + y^2 + z^2 \rangle_{tie} \qquad \text{(A22)}$$

$$\sum_{j=1}^{\infty} \langle V_0 \cdot V_j \rangle = (\delta A - \epsilon l_c)(\delta A + \epsilon l_c)/(2\epsilon) \qquad \text{(A23)}$$

where δ is the fraction of tie chains as defined above, $\epsilon = 1 - \delta$, and $A = L + l_c$ is the combined thickness of both domains. We now write $\langle R^2 \rangle = \langle R^2 \rangle_{xy} + \langle R^2 \rangle_z$, where the two latter terms represent contributions from directions parallel and perpendicular, respectively, to the lamellar plane. The xy contributions from eq A22 are the mean-square throw distances calculated above, while the z contributions are the squared distances l_c^2 or A^2. Equation A23 only contains z contributions.[26] When all the contributions are inserted and rearranged, we obtain

$$\langle R^2 \rangle_{xy} = (2/3)nL(D_1/D_2)\phi s(1 + 2\epsilon) \qquad \text{(A24)}$$

and

$$\langle R^2 \rangle_z = nA^2\delta \qquad \text{(A25)}$$

Neither of these quantities exhibits σ dependence. Therefore, both parallel and perpendicular components of the radius of gyration are predicted to be invariant to the structural changes accompanying changes in temperature.[31]

Acknowledgment. I am grateful to Dr. J. D. Hoffman for a number of helpful discussions. This research was

supported in part by the National Science Foundation, Grant No. DMR-8607708.

Registry No. Polyethylene, 8049-65-8.

References and Notes

(1) Tanabe, Y.; Strobl, G. R.; Fischer, E. W. *Polymer* **1986**, *27*, 1147.
(2) Snyder, R. G.; Schlotter, N. E.; Alamo, R.; Mandelkern, L. *Macromolecules* **1986**, *19*, 621.
(3) Hoffman, J. D.; Williams, G.; Passaglia, E. *J. Polym. Sci., Part C* **1966**, *14*, 173.
(4) Mansfield, M.; Boyd, R. H. *J. Polym. Sci., Polym. Phys. Ed.* **1978**, *16*, 1227.
(5) Mansfield, M. L. *Chem. Phys. Lett.* **1980**, *69*, 383.
(6) Skinner, J. L.; Wolynes, P. G. *J. Chem. Phys.* **1980**, *73*, 4015.
(7) Skinner, J. L.; Wolynes, P. G. *J. Chem. Phys.* **1980**, *73*, 4022.
(8) Skinner, J. L.; Park, Y. H. *Macromolecules* **1984**, *17*, 1735.
(9) Boyd, R. H. *Polymer* **1985**, *26*, 323.
(10) Boyd, R. H. *Polymer* **1985**, *26*, 1123.
(11) Syi, J. L.; Mansfield, M. L., to be published.
(12) Geil, P. H. *Polymer Single Crystals*; Wiley: New York, 1963; Chapter 5.
(13) Keller, A. *Rep. Prog. Phys.* **1968**, *31*, 623.
(14) As was pointed out by a referee, an alternative explanation for the increase in crystallinity observed by Tanabe, Strobl, and Fischer (ref 1) could be the growth of new, thinner crystallites between those already present. Standard crystallization theory (e.g., ref 19) does indeed predict that crystal thickness decreases with decreasing temperature, and so at least on that account, the growth of new, thinner crystals makes sense. If new crystals do form, then the explanation given here is, of course, invalid. Note, however, that the balance of chemical potentials discussed here, if it is achieved before the new crystals have time to appear, would prevent any new crystal growth for the same reason that crystals do not grow from the bulk melt at T_m.
(15) Treloar, L. R. G. *The Physics of Rubber Elasticity*; Oxford University Press: London, 1975.
(16) Fischer, E. W. *Kolloid-Z. Z. Polym.* **1967**, *218*, 97.
(17) Zachmann, H. G. *Kolloid-Z. Z. Polym.* **1969**, *231*, 504.
(18) Elias, H. G. *Macromolecules*, 2nd ed.; Plenum: New York, 1984; Vol 1, p 271.
(19) Hoffman, J. D.; Davis, G. T.; Lauritzen, J. I. *Treatise Solid State Chem.* **1976**, *3*.
(20) The two semiempirical low-temperature approximations $\Delta g = [\Delta h_f \Delta T/T_m]f$, for $f = 2T/(T_m + T)$ or $f = T/T_m$ (see ref 19) bring the low-temperature points in Figures 3–5 closer to the line, but discrepancies still exist. This may also be due to the known deficiencies of rubber elasticity theory at high extensions.
(21) Guttman, C. M.; DiMarzio, E. A.; Hoffman, J. D. *Polymer* **1981**, *22*, 1466.
(22) Guttman, C. M.; DiMarzio, E. A. *Macromolecules* **1982**, *15*, 525.
(23) Vonk, C. G. *J. Polym. Sci., Polym. Lett. Ed.* **1986**, *24*, 305.
(24) Mansfield, M. L.; Guttman, C. M.; DiMarzio, E. A. *J. Polym. Sci., Polym. Lett. Ed.* **1986**, *24*, 565.
(25) An earlier statement to the contrary (ref 4) is incorrect. See ref 11.
(26) Mansfield, M. L. *Macromolecules* **1986**, *19*, 851.
(27) Mansfield, M. L. *Macromolecules* **1986**, *19*, 1421.
(28) Grubb, D. T. *Macromolecules* **1985**, *18*, 2282 and references therein.
(29) The value D_2 is the correct proportionality constant in these expressions because it properly normalizes $P(t)$ in eq A11.
(30) Upon evaluating a number of the integrals in the Appendix, one encounters Fourier series whose sums can be found (or quickly derived) by consulting: Gradshteyn, I. S.; Ryzhik, I. M. *Table of Integrals, Series, and Products*; Jeffrey, A., Ed.; Academic: New York, 1980; pp 38–39.
(31) Reference 26 derives an expression for the radius of gyration in terms of the degree of crystallinity. It should be understood that that equation only applies when the amorphous domains are isotropic.

Analysis of the Temperature Quotient of the Intrinsic Viscosity of Stiff-Chain Polymers

Gandavarapu Venkataramana Reddy† and Miloslav Bohdaneckỳ*

Institute of Macromolecular Chemistry, Czechoslovak Academy of Sciences, 162 06 Prague 6, Czechoslovakia. *Received November 20, 1986*

ABSTRACT: The temperature quotient of the intrinsic viscosity, d ln $[\eta]/dT$, of stiff-chain polymers is discussed in terms of the Yamakawa–Fujii wormlike cylinder model. A method of estimating the quotient d ln $((R^2)_0/M)_\infty/dT$ is outlined and applied to the data for some cellulose derivatives (tricarbanilate, tributyrate, nitrate with 12.5% N, ethyl ether). The possibility of assessing the temperature effect on other parameters of the model (chain diameter and shift factor) is analyzed.

The temperature quotient of the intrinsic viscosity, d ln $[\eta]/dT$, of random-flight chains in the nondraining limit contains contributions from the short-range interactions and the excluded-volume effect. If appropriate corrections are applied for the latter, the temperature quotient, d ln $(\langle R^2\rangle_0/M)_\infty/dT$, of the mean-square unperturbed chain length, $\langle R^2\rangle_0$, in the random-coil limit can be estimated. This quotient is a quantity which provides important information on the energetics of the bond conformation.[1]

With stiff-chain polymers, the excluded-volume effect is usually weak, which seemingly facilitates the estimation of d ln $(\langle R^2\rangle_0/M)_\infty/dT$. Yet hydrodynamic properties of such chains do not comply with the model of nondraining random coils so that the interpretation of the quotient d ln $[\eta]/dT$ requires a special approach.

This problem is analyzed in the present paper on the basis of the theory of hydrodynamic properties of the continuous wormlike cylinder model.[2] The values of d ln $(\langle R^2\rangle_0/M)_\infty/dT$ for several cellulose derivatives are estimated, and the temperature effect on other parameters characterizing the chain in terms of this model is discussed.

Theoretical Section

The continuous wormlike cylinder model[2] is characterized by its contour length L, diameter d, and the persistence length a or the Kuhn statistical segment length $\lambda^{-1} = 2a$. The latter is connected with $(\langle R^2\rangle_0/M)_\infty$ by

$$\lambda^{-1} = (\langle R^2\rangle_0/M)_\infty M_L \quad (1)$$

where M_L is the shift factor. In terms of this model, the intrinsic viscosity $[\eta]_0$ of stiff chains unperturbed by the excluded-volume effect is[2]

†Fellow of the UNESCO Postgraduate Course in Macromolecular Chemistry. Permanent address: Leather Auxiliaries, Central Leather Research Institute, Adyar, Madras 600020, India.

0024-9297/87/2220-1393$01.50/0